Published May 2, 2005

Insulin stimulates the halting, tethering, and fusion of mobile GLUT4 vesicles in rat adipose cells

Vladimir A. Lizunov,[1,3] Hideko Matsumoto,[2] Joshua Zimmerberg,[1] Samuel W. Cushman,[2] and Vadim A. Frolov[1,3]

[1]Laboratory of Cellular and Molecular Biophysics, National Institute of Child Health and Human Development, and [2]Experimental Diabetes, Metabolism, and Nutrition Section, Diabetes Branch, National Institute of Diabetes and Digestive and Kidney Diseases, National Institutes of Health, Bethesda, MD, 20892
[3]A.N. Frumkin Institute of Electrochemistry, Russian Academy of Science, Moscow, 119071, Russia

Glucose transport in adipose cells is regulated by changing the distribution of glucose transporter 4 (GLUT4) between the cell interior and the plasma membrane (PM). Insulin shifts this distribution by augmenting the rate of exocytosis of specialized GLUT4 vesicles. We applied time-lapse total internal reflection fluorescence microscopy to dissect intermediates of this GLUT4 translocation in rat adipose cells in primary culture. Without insulin, GLUT4 vesicles rapidly moved along a microtubule network covering the entire PM, periodically stopping, most often just briefly, by loosely tethering to the PM. Insulin halted this traffic by tightly tethering vesicles to the PM where they formed clusters and slowly fused to the PM. This slow release of GLUT4 determined the overall increase of the PM GLUT4. Thus, insulin initially recruits GLUT4 sequestered in mobile vesicles near the PM. It is likely that the primary mechanism of insulin action in GLUT4 translocation is to stimulate tethering and fusion of trafficking vesicles to specific fusion sites in the PM.

Introduction

Insulin regulates glucose transport in muscle and adipose cells through the intracellular redistribution of the glucose transporter 4 (GLUT4; Cushman and Wardzala, 1980; Suzuki and Kono, 1980). GLUT4 content in the plasma membrane (PM) of adipose cells is determined by a dynamic equilibrium between its exocytosis and internalization. In basal adipose cells, the content of GLUT4 in the PM remains low (<5%) as GLUT4 internalizes 10 times faster than it is delivered to the PM (Slot et al., 1991; Satoh et al., 1993; Holman et al., 1994; Malide et al., 2000; for review see Bryant et al., 2002). Insulin considerably stimulates the rate of GLUT4 exocytosis with relatively little effect on the rate of internalization (Satoh et al., 1993; Karylowski et al., 2004). Consequently, ~50% of intracellular GLUT4 is translocated to the PM upon insulin activation, providing a >10-fold increase in the amount of transporter on the cell surface (Malide et al., 2000; for reviews see Pessin et al., 1999; Bryant et al., 2002).

GLUT4 is carried to the PM by specialized tubulovesicular compartments (referred to here as GLUT4 vesicles) tightly packed with the transporter (Rea and James, 1997). GLUT4 vesicles belong to specialized exocytic compartments actively excluding other recycling proteins (Martin et al., 1996; Malide et al., 1997; Hashiramoto and James, 2000; Lampson et al., 2001). In the basal state, the GLUT4 vesicles sequester up to 95% of the total GLUT4 in adipose cells (Martin et al., 1996; Malide et al., 1997; Lee et al., 1999). The vesicles slowly exchange GLUT4 with the rest of the intracellular pool and with the PM (Holman et al., 1994; Karylowski et al., 2004; Watson et al., 2004). The dynamics of basal GLUT4 recycling indicate that a fraction of the GLUT4 vesicles is mobile (Bryant et al., 2002). It is increasingly thought that insulin regulates the mobility of GLUT4 vesicles, yet the details and mechanisms of insulin's action remain controversial.

Live microscopy studies performed on 3T3-L1 adipocytes (3T3 fibroblast cell line that has been differentiated to adipose-like cells) demonstrate that in the basal state most of the GLUT4 vesicles remain relatively static (Oatey et al., 1997; Patki et al., 2001), although long-range movements of GLUT4 vesicles along microtubules were occasionally observed (Fletcher et al., 2000; Semiz et al., 2003). The microtubule network supports the GLUT4 translocation induced by insulin (Patki et al., 2001; Semiz et al., 2003; Karylowski et al., 2004). The disruption of the microtubular network prevents long-range movements of GLUT4 vesicles and substantially inhibits GLUT4 translocation to the PM (Fletcher et al., 2000; Patki et al., 2001). Hence, it has been suggested that insulin stimulates

V.A. Lizunov and H. Matsumoto contributed equally to this paper.

Correspondence to Joshua Zimmerberg: joshz@helix.nih.gov

H. Matsumoto's present address is Dept. of Molecular Biology, Saitama Medical School, Saitama, 350-0495, Japan.

Abbreviations used in this paper: GLUT4, glucose transporter 4; PM, plasma membrane; ROI, region of interest; TIRF, total internal reflection fluorescence; TIRFM, TIRF microscopy.

The online version of this article includes supplemental material.

Supplemental Material can be found at:
/content/suppl/2005/05/02/jcb.200412069.DC1.html

The Journal of Cell Biology, Vol. 169, No. 3, May 9, 2005 481–489
http://www.jcb.org/cgi/doi/10.1083/jcb.200412069

Published May 2, 2005

movement of GLUT4 vesicles from the cell interior toward the PM along microtubule tracks (Patki et al., 2001; Semiz et al., 2003). Translocation of the new vesicles to the PM would boost GLUT4 exocytosis because the vesicles carry essential parts of the docking/fusion machinery (Martin et al., 1996; Timmers et al., 1996; Grusovin and Macaulay, 2003).

However, in nonstimulated primary adipose cells, a fraction of all GLUT4 vesicles is already located near the PM. Even in 3T3-L1 adipocytes, where GLUT4 is mainly concentrated in the perinuclear region (Patki et al., 2001), GLUT4-containing vesicles were also reportedly found near the PM (Oatey et al., 1997). These peripheral vesicles were suggested to be an initial source of GLUT4 translocated to the PM upon insulin stimulation (Fletcher et al., 2000; Semiz et al., 2003), although it has never been directly demonstrated. In primary adipose cells, the disperse cytoplasmic GLUT4 vesicles already make up a majority of the GLUT4-containing compartments (Lee et al., 1999; Malide et al., 2000). In freshly isolated primary adipose cells, the GLUT4 vesicles are uniformly spread over the whole cytoplasm with many of the vesicles located near the PM (Slot et al., 1991; Malide et al., 1997, 2000). Such spatial distribution of GLUT4 in basal primary adipose cells immediately suggests that GLUT4 vesicles proximal to the PM play an essential role in the insulin response in these cells. However, the dynamics of these GLUT4 vesicles in primary adipose cells remain unknown.

Recently, insulin has been shown to stimulate translocation of effector molecules providing specific targeting of GLUT4 vesicles to the PM (Grusovin and Macaulay, 2003; Inoue et al., 2003; Saltiel and Pessin, 2003). Thus, insulin may be involved in regulating tethering of GLUT4 vesicles located near the PM. To test this hypothesis, we designed an approach to visualize the dynamic behavior of GLUT4 vesicles located near the PM in primary adipose cells using total internal reflection fluorescence (TIRF) microscopy (TIRFM). Here, we report the resolution of the movements, docking, and fusion of single GLUT4 vesicles, in both the basal and insulin-stimulated states. We find that without insulin GLUT4 vesicles rapidly traffic near the PM along stationary trajectories formed by a microtubule network covering the entire PM, although GLUT4 vesicles transiently stop and loosely tether to the PM. Insulin stops this traffic, tightly tethering vesicles at the PM where they form clusters. After fusion, the slow diffusion of GLUT4 from clustered vesicles determines the overall increase of PM GLUT4. We conclude that one of the primary modes of insulin action on adipose cells is to halt a hitherto unrecognized form of GLUT4 trafficking that scans the cytoplasmic surface of a cell membrane, and then stimulates tethering and fusion of vesicles bearing glucose transporters into the cell membrane.

Results

In isolated adipose cells, GLUT4 vesicles are scattered near the PM

When isolated from tissue, white adipose cells are round and their interior is filled with a large droplet of stored triglyceride (Fig. 1, A and B), leaving a thin (1–3-μm) layer of cytoplasm between the lipid droplet and the PM (Cushman, 1970; Malide et al., 2000). In our experiments, these cells, which ordinarily float in their medium, were slightly pressed against the coverslip such that a small flattened part of the PM and nearby cytoplasm (hereafter termed the "TIRF zone") was illuminated by the evanescent wave (Fig. 1 B and Fig. S1 A, available at http://www.jcb.org/

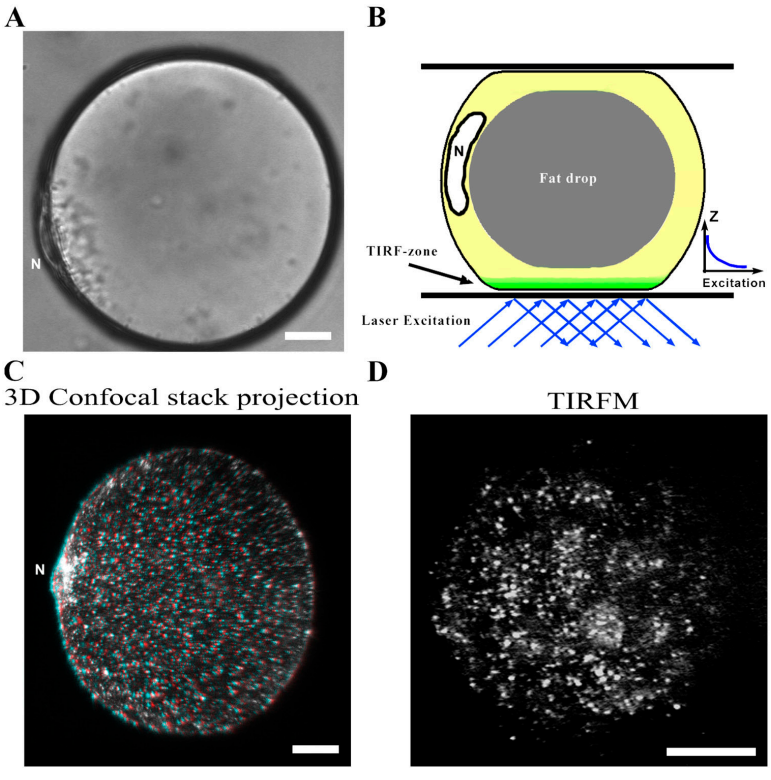

Figure 1. **Confocal microscopy and TIRFM of isolated white adipose cells.** (A) Differential interference contrast image of an isolated cell slightly squashed between two coverslips with nuclear region facing to the left side. (B) Flat round region of PM and adjacent thin layer of cytoplasm accessible for TIRF imaging (TIRF zone). (inset) Under TIRF illumination the fluorescence excitation intensity decreases exponentially with distance from the coverslip. (C) Three-dimensional reconstruction of confocal images of a basal adipose cell transfected with GLUT4-GFP. Use red and green glasses to view this image. (D) Randomly selected part of basal adipose cell visualized with TIRF. Substantial amounts of GLUT4 vesicles are located near the PM (within 400 nm; see Materials and methods) in randomly scattered fashion. Note the variation of fluorescence intensity of vesicles due to different positions relative to the coverslip. Bars, 10 μm.

Published May 2, 2005

cgi/content/full.200412069/DC1). The three-dimensional distribution and dynamics of GLUT4 vesicles in the cytoplasm of basal cells was characterized by confocal and TIRFM.

The HA-GLUT4-GFP construct expressed in these cells (Dawson et al., 2001) was seen in distinct bright fluorescent spots (Fig. 1, C and D). This punctate pattern of GLUT4 distribution is consistent with the previous observations that up to 95% of intracellular GLUT4 is stored in vesicles (Lee et al., 1999; Malide et al., 2000). Confocal microscopy showed that for most of the transfected cells cultured overnight the punctate patterns of GLUT4 distribution (Fig. 1 C) resemble those of freshly isolated cells; i.e., GLUT4 predominantly resides in vesicles scattered over the whole cytoplasm (Malide et al., 1997). However, with increasing time in culture (>24 h), the bulk of the fluorescence starts to relocate to the perinuclear region (unpublished data). We used cells that were incubated overnight, but within 24 h after isolation; we selected those cells with substantial amounts of fluorescent vesicles scattered throughout the cytoplasm.

Analysis of TIRFM images showed a similar punctate pattern of GLUT4 distribution (Fig. 1 D), demonstrating that the spots mostly corresponded to single GLUT4 vesicles (see Material and methods). In the basal state, we detected 15.7 ± 3.2 vesicles per a 100-μm^2 area of the PM (65 cells, SD) in the TIRF zone. The proximity of many GLUT4 vesicles to the PM is consistent with earlier papers on GLUT4 distribution in adipose cells in primary culture (Lee et al., 1999; Malide et al., 2000).

GLUT4 vesicles near the PM are highly mobile

Time-lapse videos made using TIRFM demonstrated a high basal trafficking of GLUT4 vesicles in the vicinity of the PM (Video 1, available at http://www.jcb.org/cgi/content/full.200412069/DC1). To quantify this traffic, we used a projection algorithm producing distinct traces (Fig. 2 A) for all moving vesicles in the TIRF zone. In basal cells, we detected on average 10.0 ± 1.4 traces/100 μm^2/min (22 cells, SD) representing trajectories of moving vesicles. The vesicles often underwent long-range (>10 μm) lateral movements, presumably approaching the PM along the way (as deduced from periodic increases in vesicle fluorescence). Vesicles tended to stop for a period of time (varying from a fraction of a second to 100 s) at dedicated places, and sometimes two or more vesicles stopped at the same location. Ultimately, vesicles exited the TIRF zone laterally or in a direction perpendicular to the coverslip (for a detailed description, see the section Kinetic analysis of GLUT4 recycling in primary adipose cells in the online supplemental material).

Moving vesicles took predefined trajectories. Often, vesicles followed exactly the same trajectories one after another (Fig. 2 B and Video 2, available at http://www.jcb.org/cgi/content/full.200412069/DC1l). In adipose cells transfected with fluorescent tubulin, we observed an extensive microtubular network (Fig. S1 B; Malide and Cushman, 1997). Long microtubular pathways (>30 μm) that cover the entire cytoplasm (Fig. S1 B)

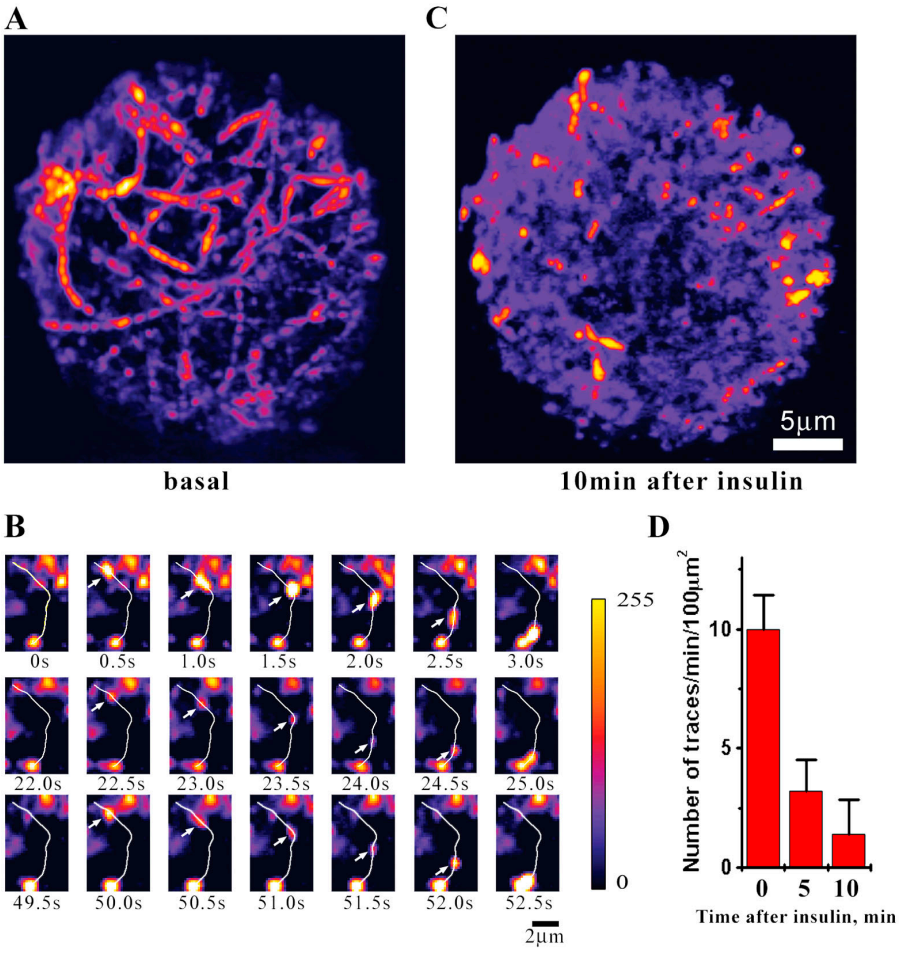

Figure 2. **Traffic of GLUT4 vesicles in adipose cells in the basal and insulin-stimulated states.** Time-lapse TIRF images were projected onto a single plane to visualize vesicle movements. (A) Projection image of a cell in the basal state made from a 1-min-long recording (Video 1, available at http://www.jcb.org/cgi/content/full/jcb.200412069/DC1). (B) Sequential frames show three vesicles (arrows) taking the same pathway (white line). See Video 2. (C) Projection image of a cell taken 10 min after insulin application. Note that both the number of traces and the average running distance for GLUT4 vesicles are significantly reduced compared with the basal state. Fluorescence intensity is shown in pseudocolor. (D) Quantification of traffic for cells in the basal state and cells 5 and 10 min after insulin application. Data represent mean number of traces detected per 100 μm^2/min from at least 20 cells in each state.

Published May 2, 2005

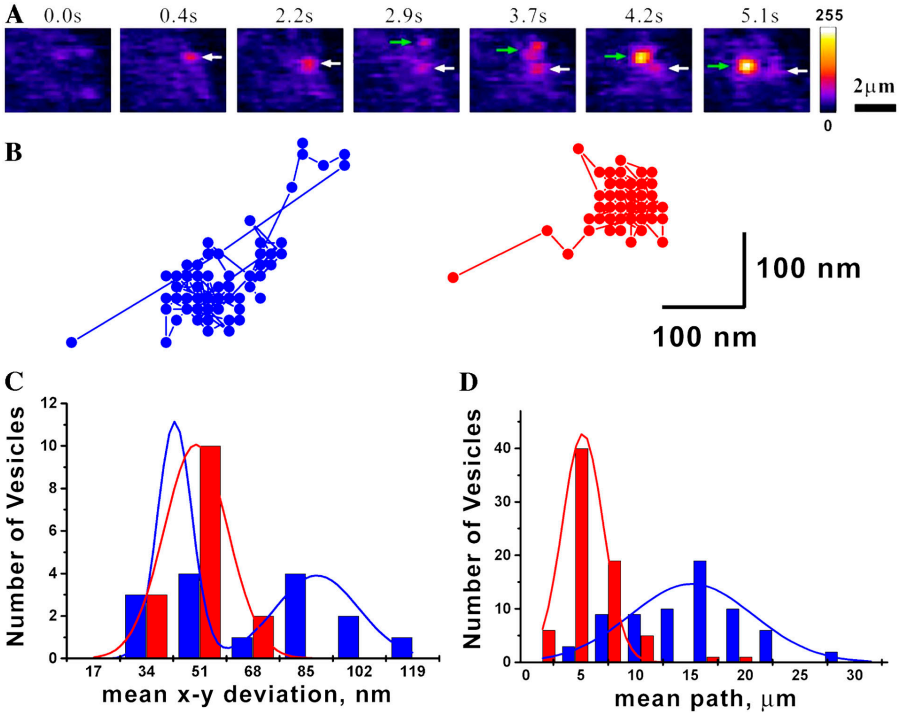

Figure 3. **Tethering of mobile GLUT4 vesicles to the PM of primary adipose cells.** (A) Sequential frames show two GLUT4 vesicles (arrows) approaching and quickly tethering to the PM. (B) Examples of trajectories (projected onto the x-y "coverslip" plane) of GLUT4 vesicles tethering to the PM in the basal (blue) and insulin-stimulated (red) states; each point corresponds to the center of the vesicle ROI. (C) Histograms of SD of vesicle position from the point of tethering in the x-y plane (amplitude of "wiggling" = $\sqrt{(SD_x + SD_y)}$); ~100 consecutive frames were used for the SD calculation for each vesicles; blue, vesicles in the basal state; red, vesicles in the insulin-stimulated state (10 min after insulin treatment). (D) Histograms of the distances a GLUT4 vesicle travels until the first stop in the basal (blue) and insulin-stimulated (red) states.

could very well account for the observed movements of GLUT4 vesicles. Indeed, the GLUT4 vesicles closely follow the paths marked by fluorescent tubulin (Video 3, available at http://www.jcb.org/cgi/content/full.200412069/DC1; Semiz et al., 2003). The distribution of vesicle velocity exhibits two distinct peaks at 0.6 and ~2 μm/s (Fig. S1 C), both falling into the range of velocities characteristic for fast kinesin or dynein motors (Higuchi and Endow, 2002; Ma and Chisholm, 2002).

Insulin stimulates tethering of mobile GLUT4 vesicles to the PM

In stimulated cells we observed a drastic reduction in the traffic (Video 4, available at http://www.jcb.org/cgi/content/full.200412069/DC1). Only 1.4 ± 1.4 traces/100 m^2/min (18 cells, SD) were detected 10 min after the insulin treatment, approximately eightfold less compared with the basal state (Fig. 2, C and D). Our analysis indicates that the reduction of the traffic is due to immobilization of GLUT4 vesicles at the PM. First, upon insulin stimulation, GLUT4 vesicles attach to the PM much tighter. Fig. 3 A shows two GLUT4 vesicles that attached to the PM shortly after appearance in the TIRF zone. After attachment, the vesicles do not "wiggle" near the point of attachment (Li et al., 2004) as much in the presence of insulin as they do in the basal state; the amplitude of wiggling has two peaks (42 ± 11 and 88 ± 26 nm, $n = 15$, SD) in the basal state, whereas in the insulin-stimulated state, only the first peak (49 ± 20 nm, $n = 15$, SD, statistically indistinguishable from the first "basal" peak) is present (Fig. 3, B and C). Thus, insulin stimulation almost completely eliminates the long-range "wiggling" of the attached vesicles. Moreover, these vesicles rarely move again and so the mobile vesicles all remain in the TIRF zone. Second, insulin diminished the distance traveled by the vesicles in the TIRF zone (from 15 ± 6 to 5 ± 2 μm, $n = 70$, SD; Fig. 3 D). Thus, insulin stimulates tighter and quicker attachment of mobile GLUT4 vesicles to the PM of adipose cells (see Fig. S4, available at http://www.jcb.org/cgi/content/full.200412069/DC1, and the section Kinetic analysis of GLUT4 recycling in primary adipose cells in the online supplemental material).

Insulin immobilizes GLUT4 vesicles into clusters on the PM

Although the initial distribution of GLUT4 vesicles around the cell surface is relatively uniform (Fig. 1, C and D), we observed that insulin stimulates formation of fluorescent domains alternating with dark regions (Fig. 4, A and C). To characterize the degree of nonuniformity of the spatial distribution of GLUT4 vesicles near the PM, we applied a pair-distance correlation analysis. Insulin-stimulated cells showed a distinct peak on the pair-distance correlation curve (Fig. 4 B), demonstrating that a significant percentage of vesicles are clustered. The width of the main peak gives an estimate of average cluster size (~5 μm). Pair-distance correlations obtained with cells in the basal state exhibited no significant deviation from a randomly scattered point distribution (all points lie inside the 99% confidence interval), as tested by simulation. These observations are consistent with previous studies that insulin targets GLUT4 vesicles to specific places of the PM of 3T3-L1 adipocytes (Patki et al., 2001; Semiz et al., 2003). Moreover, insulin signaling in adipose cells has been proposed to be associated with specific domains of the PM (Saltiel and Pessin, 2003). If insulin promotes tethering of GLUT4 vesicles to the PM, then to complete the insulin response docked vesicles must fuse to release GLUT4 to the PM. We further confirmed that insulin stimulates tethering and fusion of GLUT4 vesicles to the PM within the characteristic time of the appearance of GLUT4 in the PM reported previously (Dawson et al., 2001; Tengholm and Meyer, 2002).

Published May 2, 2005

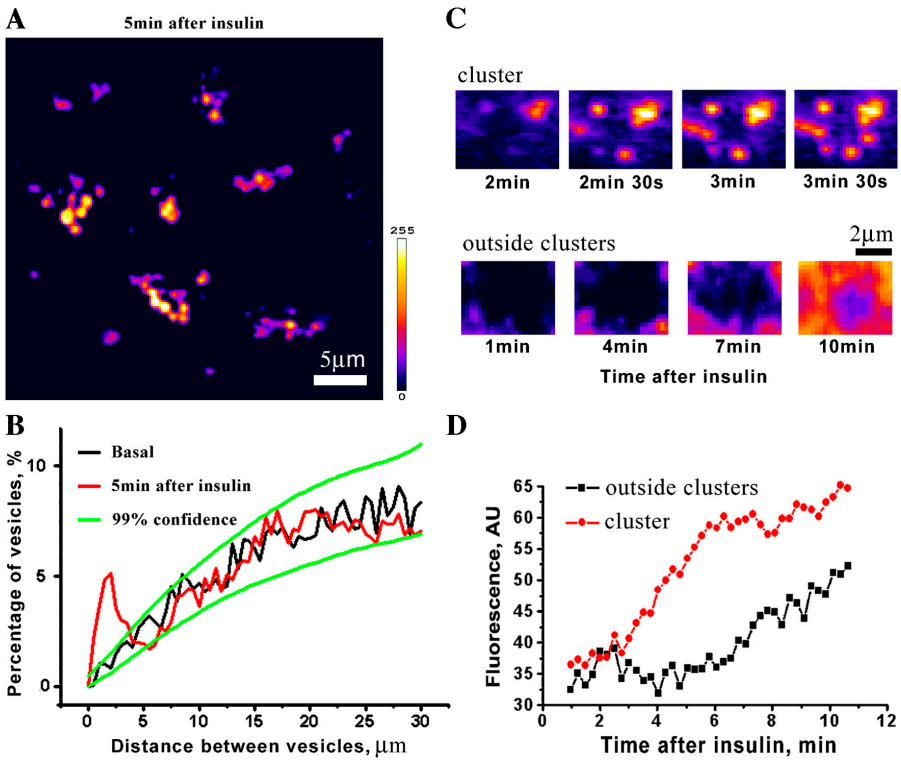

Figure 4. **Clustering of GLUT4 vesicles near PM after application of insulin in adipose cells.** (A) TIRF image of a cell 5 min after insulin stimulation. (B) Pair-distance correlation functions of vesicle distributions for cells in the basal and insulin-stimulated states. With insulin (red curve) this function exhibits a peak in the range of 1–5 μm, and shows that a significant fraction of vesicles are clustered. The correlation function for cells in the basal state (black) revealed no statistically significant deviation from the random distribution. Green curves represent the 99% confidence interval for spatially random distribution acquired by computer simulation. (C) Sequential images show arrival of new vesicles to a cluster (top) and subsequent redistribution of GLUT4 to adjacent regions outside the cluster (bottom). (D) Time course of fluorescence integrated over (red) and outside (black) the cluster.

GLUT4 vesicles fuse with the PM shortly after docking in clusters

Formation of clusters was already seen after 2 min of insulin treatment (Fig. 4 C, top). Shortly after, we saw an increase of GLUT4 fluorescence between the clusters, where no vesicles were detected (Fig. 4 C, bottom). The time lag between the increase of fluorescence integrated over the cluster region (Fig. 4 D, red curve) and over the dark region (Fig. 4 D, black curve) was several minutes. That fluorescence redistributes from clusters to the dark regions of the PM strongly indicates that vesicles in the clusters fuse to the PM. We confirmed the appearance of GLUT4 on the PM by antibody labeling; moreover, wortmannin, known to interfere with insulin signaling, ablated the translocation of GLUT4 to the PM (Fig. S2, A and B, available at http://www.jcb.org/cgi/content/full.200412069/DC1; Dawson et al., 2001). Next, we analyzed the dynamics of GLUT4 release from individual vesicles tethered to the PM.

In insulin-stimulated cells, GLUT4 vesicles lost their fluorescence shortly after attachment; the vesicles approached the PM and stopped, and then the vesicle fluorescence dimmed. Fig. 5 A demonstrates the fluorescence spreading from the same GLUT4 vesicle indicated by the green arrow in Fig. 3 A

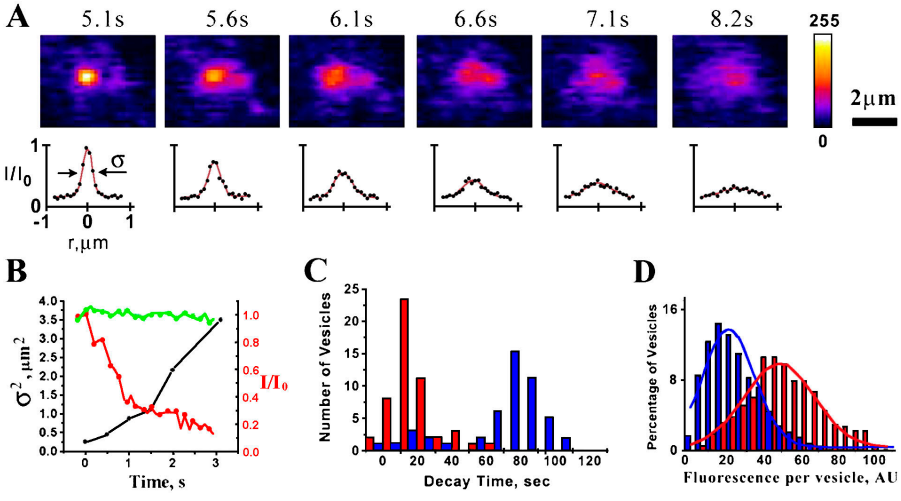

Figure 5. **Fusion of single GLUT4 vesicles in adipose cells.** (A) Image sequence (top) showing fusion of the vesicle from Fig. 3 A (green arrow) detected by the spreading of GLUT4 (Video 5, available at http://www.jcb.org/cgi/content/full/jcb.200412069/DC1). Gaussian fit (bottom) of the vesicle fluorescence radial intensity profile shows a decrease of peak intensity and simultaneous radial widening of the profile (σ represents full-width half-maximum). (B) Time course of peak width (black) and peak intensity (red) acquired from the Gaussian fit, and total fluorescence integrated over a circular region (4-μm-diam) surrounding the vesicle (green); the total fluorescence (green) remains constant as the vesicle diameter (40 nm) is significantly smaller than the characteristic penetration length of the evanescent wave (Loerke et al., 2002). All intensities are normalized to their initial values. (C) Histogram of the time of vesicle fluorescence decay (τ) for insulin-stimulated (red) and basal (blue) cells. The values of τ were obtained by exponential fit of fluorescence time course. In basal cells, the average time of fluorescence decay (77 ± 13 s) was statistically indistinguishable from the rate of bleaching (80 ± 10 s). (D) Vesicle fluorescence before (blue, 23 ± 14 AU, SD, n = 423) and 15 min after (red, 48 ± 18 AU, SD, n = 398) insulin application. The increased brightness indicates closer proximity to the PM as the vesicle fluorescence decreases exponentially with distance from the PM (Fig. 1 B, inset).

Published May 2, 2005

to the PM; the corresponding radially symmetric Gaussian fits of the fluorescence intensity are placed below each frame (Video 5, available at http://www.jcb.org/cgi/content/full.200412069/DC1). The fits demonstrate that while the peak fluorescence decayed (Fig. 5 B, red curve), the profile of vesicle fluorescence widened (Fig. 5 B, black curve) but the total amount of fluorescence in the circular region (4 μm in diameter) surrounding the vesicle remained constant (Fig. 5 B, green curve), verifying that the vesicle underwent fusion rather than moved away from the PM (Loerke et al., 2002).

The coefficient of lateral diffusion of GLUT4 from such immediate fusion events can be estimated as 2×10^{-9} cm^2/s from the kinetics of the fluorescence profile widening (Fig. 5 B, black curve; Schmoranzer et al., 2000). Using FRAP, we obtained a similar estimate of the diffusion coefficient of GLUT4 in the PM, 1.4×10^{-9} cm^2/s (Fig. S3 A, available at http://www.jcb.org/cgi/content/full.200412069/DC1), thus pointing out that GLUT4 vesicles can quickly release the transporter to PM. However, the quick unrestricted release of GLUT4 corresponding to detectable widening of the fluorescence profile, as in Fig. 5 A, was detected only rarely. We estimated the characteristic times of GLUT4 release from individual fusing vesicles by an exponential fit of the decay of vesicle fluorescence (as in Fig. 5 B, red curve). Fig. 5 C demonstrates that most of the vesicles release GLUT4 much slower than 1 s, the estimated characteristic time of unrestricted release calculated from the above diffusion constant (Fig. 5 B). Yet, Fig. 5 C shows that the decay of the vesicle fluorescence was indeed due to insulin stimulation: insulin-stimulated vesicles lose fluorescence much faster (in 20 ± 12 s) than vesicles in the basal state (in 77 ± 13 s). A decay time slower than 70 s was statistically indistinguishable from the characteristic time of vesicle bleaching under constant laser illumination (80 ± 10 s). In control experiments performed on cells in the basal state using intermittent illumination, no fluorescence decay was detected for most of the vesicles, confirming that bleaching was the reason for the slow decay ($\tau > 70$ s). Because fluorescence is not lost but redistributes in times substantially faster than 70 s, these data further confirm that insulin-stimulated tethering of GLUT4 vesicles in clusters is followed by fusion of the vesicles with the PM. Fig. 5 C also shows that the fluorescence of a small fraction of vesicles in nonstimulated cells (Fig. 5 C, blue bars) decayed quickly, indicating fusion events in the basal state. These rare exocytic events can account for slow basal recycling of GLUT4 (Holman et al., 1994; Karylowski et al., 2004).

Insulin changes both the kinetic behavior and the spatial distribution of GLUT4 vesicles in the TIRF zone. Within 15 min of insulin treatment, the vesicles moved into clusters (Fig. 4 A) and became closer to the PM (Fig. 5 D). Thus, insulin initially mobilized vesicles in the TIRF zone, relocating them to fusion sites on the PM. New GLUT4 vesicles that are being constantly formed to replenish the vesicle population provide GLUT4 to the PM (Bryant et al., 2002). Fig. 2 D demonstrates that vesicle movements are infrequently detected 10 min after insulin stimulation, when the new nontrafficking distribution of GLUT4 is established (Holman et al., 1994). We suggest that these short movements of GLUT4 vesicles in the steady-state after insulin treatment represent the same pathways that vesicles take in the basal state. However, the average vesicle displacement is much shorter because the probability of irreversible attachment to the PM, mostly leading to fusion (Fig. S4 and the section Kinetic analysis of GLUT4 recycling in primary adipose cells in the online supplemental material), is dramatically augmented by insulin.

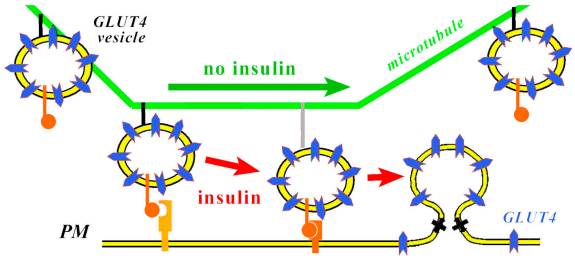

Figure 6. **Hypothetical mechanism of insulin-stimulated recruitment of GLUT4 vesicles to fusion sites in the PM.** In the basal state, most of the GLUT4 is in vesicles that move on microtubules along the PM passing available fusion sites. Insulin via intracellular signaling cascade stimulates tethering of GLUT4 vesicles to the first encountered fusion site; the fusing vesicles accumulate in clusters in the PM. The release of GLUT4 from fusing vesicles is restricted (see text) in ways that may be regulated.

Our kinetic model of GLUT4 recycling (see the online supplemental material) indicates that insulin augments both the probability of tethering at specific fusion sites and the subsequent priming of the vesicles leading to their fusion to the PM. In insulin-stimulated cells, the GLUT4 vesicles are expected to fuse at the first encountered fusion site as typical cargo vesicles (Schmoranzer and Simon, 2003). The probability of fusion is much less in nonstimulated cells; thus, mobile GLUT4 vesicles bypass many fusion sites, remaining on the microtubule network for a long time. Fig. 6 summarizes our model for the insulin stimulation of GLUT4 exocytosis. Upon formation, the GLUT4 vesicles move on microtubules until they fuse, like vesicles delivering constitutive post-Golgi cargo (Schmoranzer and Simon, 2003). The GLUT4 vesicles fuse to the PM at special fusion sites, with the probability of tethering and fusion being regulated by insulin.

Discussion

It has long been known that in primary adipose cells GLUT4 is predominantly sequestered in specialized vesicles uniformly scattered over the cytoplasm (Lee et al., 1999; Malide et al., 2000). Such a uniform distribution was shown to be characteristic of freshly isolated cells; with increasing time in culture, GLUT4 vesicles tend to relocate to the perinuclear region (Malide et al., 1997). However, it has remained unclear whether these scattered GLUT4 vesicles, especially those situated relatively close to the PM (Lee et al., 1999; Malide et al., 2000), represent a static pool, awaiting insulin stimulation to trigger fusion of the vesicles to the PM, or a dynamic pool constantly exchanging GLUT4. We demonstrate here that in freshly isolated adipose cells, GLUT4 vesicles located near the PM are mobile. The vesicles move along microtubules, thus scanning the extensive microtubule network that densely un-

Published May 2, 2005

derlies the entire PM (Malide and Cushman, 1997). Accordingly, the mean velocities of the mobile vesicles correspond well to those reported for microtubule-based transport. The first characteristic velocity of ~0.6 μm/s corresponds to that reported for GLUT4 vesicles driven by conventional kinesin on microtubules in 3T3-L1 cells (Semiz et al., 2003). The second one, ~2 μm/s, which represents rapid, long-range movements of GLUT4 vesicles, falls into the range of velocities characteristic for fast kinesin or dynein motors (Higuchi and Endow, 2002; Ma and Chisholm, 2002). The combination of fast and slow movements, alternating with periods of idling, results in a seemingly random distribution of GLUT4 vesicles over the microtubule network (Fig. 1, C and D). Hence, white adipose cells appear to use microtubules extensively to support trafficking of GLUT4 vesicles, which is consistent with the general idea of the microtubular network supporting transport of post-Golgi vesicles to the PM (Schmoranzer and Simon, 2003).

Importantly, our data indicate that the network architecture plays an important role in the regulation of GLUT4 translocation to the PM (Fletcher et al., 2000; Semiz et al., 2003). In the basal state, GLUT4 vesicles often move close to the PM where the microtubules do (Schmoranzer and Simon, 2003). Although the vesicles stop at such sites, they are weakly tethered (Fig. 3) and ultimately escape, only rarely fusing with the PM. However, upon insulin stimulation, the tethering becomes much tighter (Fig. 3) and the vesicles accumulate in clusters (Fig. 4) in very close proximity to the PM (Fig. 5 D). The clustering likely takes place at the point of microtubule attachment to the PM as GLUT4 vesicles appear to move on the microtubules until they tether and fuse (Schmoranzer and Simon, 2003). Furthermore, clustering may also correspond to the insulin signal initiation sites proposed by Saltiel and Pessin (2003), to which various effector molecules, including molecular tethers, could be recruited. Transformations of the actin network in the periphery of adipose cells could also play a role in localization of vesicle fusion at specific sites (Malide and Cushman, 1997; Saltiel and Pessin, 2003).

In insulin-stimulated adipose cells, GLUT4 vesicles reaching the PM are quickly recruited and the long-range vesicle movements are thus halted. Contrary to this finding, in 3T3-L1 cells, insulin stimulates long-range movements of GLUT4 vesicles toward the PM, rather than inhibiting trafficking (Patki et al., 2001; Semiz et al., 2003). The discrepancy could be due to different basal distributions of GLUT4. If the distribution is shifted to the perinuclear region, as is characteristic of 3T3-L1 cells (Patki et al., 2001), then more long-range trafficking would be expected to bring these vesicles to the PM. If a substantial amount of GLUT4 vesicles is already near the PM (Slot et al., 1991; Malide et al., 2000), as in adipose cells in primary culture (Fig. 1 D), then the GLUT4 vesicles need only move slightly toward the PM to augment the rate of GLUT4 exocytosis.

Our data indicate that adipose cells might also have a means of regulating GLUT4 release at the level of the individual GLUT4 vesicle: GLUT4 is not freely released from the fusing vesicles. The release may be constrained by the trapping of GLUT4 by TUG (tether, containing a UBX domain, for GLUT4; Bogan et al., 2003) or other factors involved in packing vesicles with the transporter might interfere with GLUT4 release. Alternatively, GLUT4 may be constrained by the fusion pore, as seen for lipid dyes in small fusion pores induced by influenza HA (Zimmerberg et al., 1994; Frolov et al., 2000). We cannot determine the delay in fusion after tethering, but this gradual release of GLUT4 obviously must come after a fusion pore forms between the vesicle and the PM. If the fusion pore were sufficiently large, extracellular glucose could access the GLUT4 constrained in the fusing vesicles. These clustered transporters would contribute to the cell's glucose uptake, which is consistent with the fact that insulin stimulates glucose uptake in adipose cells maximally in 5–10 min (Vega and Kono, 1979; Satoh et al., 1993). Importantly, GLUT4 trapped in a slowly fusing vesicle cannot be retrieved from the PM via normal endocytosis. Thus, the constrained fusion may explain the overshoot of the PM GLUT4 seen after insulin application (Bogan et al., 2001; Zeigerer et al., 2002). The constrained release of cargo proteins from fused vesicles, also observed for VAMP, CDC63, and Dopamine-β-hydroxylase, could be the general mechanism of regulated redistribution of granule membrane proteins to the PM (Allersma et al., 2004).

In summary, we propose that GLUT4 vesicles follow common pathways of constitutive exocytosis, exploiting microtubule tracks on their way to the PM and revealing constrained release of membrane cargo. However, the probability of tethering and fusion of these vesicles to the PM is specifically sensitive to insulin. Insulin is known to stimulate constitutive exocytosis in general (Bryant et al., 2002), though to a lesser extent than GLUT4 exocytosis. Molecular mechanisms providing the specificity of insulin action on the GLUT4 vesicles remain to be established.

Materials and methods

Cells

White adipose cells were isolated from the epididymal fat pads of 180–250-g male rats (CD strain; Charles River Laboratories), and then transfected with 8 mg/ml HA-GLUT4-GFP plasmid, and in some experiments supplemented with 0.25 mg/ml tubulin-GFP plasmid as described previously (Malide et al., 1997; Dawson et al., 2001). Tubulin-GFP plasmid was provided by A. Tsvetkov (University of Illinois College of Medicine, Chicago, IL). Coverslips coated with poly-L-lysine were placed on the surface of the medium containing the cells shortly after the transfection. A portion of floating adipose cells spontaneously adhered to the coverslip after overnight incubation at 37°C with 5% CO_2 in DME containing 3.5% BSA (fraction V; Intergen) as described in Malide et al. (1997). Cells were stimulated with 67 nM (10 mU/ml) insulin added to the extracellular medium.

Confocal microscopy and TIRFM

A coverslip with adhered cells was placed into Delta-TPG dish (Bioptechs) in Krebs-Ringer bicarbonate Hepes buffer, pH 7.4, containing 200 nM adenosine and 5% BSA (Al-Hasani et al., 1998), supplemented with 2% Ficoll to avoid cell damaging. The cells were slightly squashed between the coverslip and the bottom of the dish (Fig. 1, A and B). All experiments were performed at 37°C maintained by Delta T4 temperature controller (Bioptechs). Confocal microscopy was performed on a microscope (model LSM510; Carl Zeiss MicroImaging, Inc.) using a 100× 1.4 NA oil-immersion objective. Stacks of confocal images were collected from each cell and three-dimensional reconstructions were performed by Imaris software (Bitplane). The Prism-less TIRFM setup (Schmoranzer et al., 2000) was based on a microscope (model IX-70; Olympus) equipped with a 60× 1.45 NA objective (Olympus), argon laser (488 nm; Spectra Physics), and intensified CCD camera (VE1000SIT; MTI). Images were digitized by acquisition board (Flashbus; Integral Technologies) controlled by MetaMorph (Universal Imaging Corp.). Time-lapse images were acquired at

Published May 2, 2005

high rates (10–30 frames/s) to monitor vesicle trafficking and fusion and at slow rates (<0.5 frames/s) to monitor changes of total fluorescence from an area of the PM. For the slow acquisition, a mechanical shutter (UniBlitz D122; Vincent Associates) synchronized with the MetaMorph software was used to block laser illumination between frames. Penetration depth d of the evanescent field was measured to be 180 ± 20 nm by a calibration procedure with 40-nm fluorescent beads attached to the piezo-driven micropipette.

Image analysis

Stacks of time-lapse images were processed using projection algorithms implemented in ImageJ 1.32 (National Institutes of Health). Mean projection image of a stack was subtracted from its max projection image to obtain the traces of all moving vesicles. The number of traces (length >2 μm) within a square region of interest (ROI) of 100 μm^2 was counted visually. The Gaussian fit of radial pixel intensity profile showed that for the moving vesicles 90% of fluorescence was confined within a circular vesicle ROI of 3 pixels. Thus, bright spots were counted as vesicles if (a) the pixel intensity profile had a local maximum and (b) the average intensity in the vesicle ROI positioned on the maximum was 20% higher than the background fluorescence. The thickness of the layer where we could detect single vesicles was ~400 nm. To measure intensity of the vesicle fluorescence, images were first background subtracted using a rolling-ball algorithm (ImageJ) with a 10-pixel radius; and then the fluorescence intensity was calculated as a sum of all pixels values in the vesicle ROI.

The degree of vesicle clustering after application of insulin was estimated by pair-distance correlation analysis. Coordinates of the peak intensity of the vesicle ROI were taken as vesicle coordinates and transferred in ASCII format to Maple (Waterloo Maple Inc.). Custom written macros counted the number of vesicles within a certain distance r (running from 0.5 to 30 μm) from each vesicle and built the cumulative frequency distribution of all vesicle-vesicle distances:

$$K(r) = n^{-2} A \sum_{i}^{n} \sum_{j \neq i}^{n} I_r(d_{ij}),$$

where n is the total number of vesicles, A is the region area, and I_r is a counter variable that is set to one if the distance between vesicles i and j $d_{ij} \leq r$, otherwise $I_r = 0$. For the analysis, circular regions of 30-μm-radius were selected from TIRF images of the cells. Because the cumulative functions were built for the same boundary conditions and were normalized over the number of vesicles, it allowed us to average it between different cells. To compare the vesicle distribution with a random spatial distribution, the random point patterns were generated by computer simulation. 30 simulations were performed using a region with the same boundary conditions and with the number of random points equal to the average amount of vesicles in the ROI defined on cells. The SD and confidence intervals were approximated from simulations of complete random spatial distributions.

Online supplemental material

Online supplemental material describes in detail the imaging of the microtubular network in adipose cells, immunofluorescence of GLUT4 exposure on cell surface, and FRAP analysis of GLUT4 mobility in the PM. Videos 1 and 2 show traffic of GLUT4 vesicles in adipose cells in the basal state, and Video 3 demonstrates the movement of the vesicles on fluorescent microtubule tracks. Video 4 shows the traffic reduced by insulin stimulation. Video 5 shows a docking-fusion event and release of GLUT4 to the PM. Fig. S1 shows the TIRFM image of the PM in the TIRF zone, the microtubular network, and a histogram of vesicle velocities. Fig. S2 shows colocalization of immunofluorescence to surface GLUT4 in the PM after application of insulin and in control experiments with wortmannin. Fig. S3 shows the analysis of the GLUT4 diffusion, whereas Fig. S4 and Table S1 describe the kinetic model of GLUT4 recycling in primary adipose cells. Online supplemental material is available at http://www.jcb.org/cgi/content/full/jcb.200412069/DC1.

The authors would like to thank Mary Jane Zarnowski for assistance in isolation and transfection of rat adipose cells.

Submitted: 10 December 2004
Accepted: 17 March 2005

References

Al-Hasani, H., C.S. Hinck, and S.W. Cushman. 1998. Endocytosis of the glucose transporter GLUT4 is mediated by the GTPase dynamin. *J. Biol. Chem.* 273:17504–17510.

Allersma, M.W., L. Wang, D. Axelrod, and R.W. Holz. 2004. Visualization of regulated exocytosis with a granule-membrane probe using total internal reflection microscopy. *Mol. Biol. Cell.* 15:4658–4668.

Bogan, J.S., A.E. McKee, and H.E. Lodish. 2001. Insulin-responsive compartments containing GLUT4 in 3T3-L1 and CHO cells: regulation by amino acid concentrations. *Mol. Cell. Biol.* 21:4785–4806.

Bogan, J.S., N. Hendon, A.E. McKee, T.S. Tsao, and H.F. Lodish. 2003. Functional cloning of TUG as a regulator of GLUT4 glucose transporter trafficking. *Nature.* 425:727–733.

Bryant, N.J., R. Govers, and D.E. James. 2002. Regulated transport of the glucose transporter GLUT4. *Nat. Rev. Mol. Cell Biol.* 3:267–277.

Cushman, S.W. 1970. Structure–function relationships in the adipose cell. I. Ultrastructure of the isolated adipose cell. *J. Cell Biol.* 46:326–341.

Cushman, S.W., and L.J. Wardzala. 1980. Potential mechanism of insulin action on glucose transport in the isolated rat adipose cell. Apparent translocation of intracellular transport systems to the plasma membrane. *J. Biol. Chem.* 255:4758–4762.

Dawson, K., A. Aviles-Hernandez, S.W. Cushman, and D. Malide. 2001. Insulin-regulated trafficking of dual-labeled glucose transporter 4 in primary rat adipose cells. *Biochem. Biophys. Res. Commun.* 287:445–454.

Fletcher, L.M., G.I. Welsh, P.B. Oatey, and J.M. Tavare. 2000. Role for the microtubule cytoskeleton in GLUT4 vesicle trafficking and in the regulation of insulin-stimulated glucose uptake. *Biochem. J.* 352:267–276.

Frolov, V.A., M.S. Cho, P. Bronk, T.S. Reese, and J. Zimmerberg. 2000. Multiple local contact sites are induced by GPI-linked influenza hemagglutinin during hemifusion and flickering pore formation. *Traffic.* 1:622–630.

Grusovin, J., and S.L. Macaulay. 2003. Snares for GLUT4—mechanisms directing vesicular trafficking of GLUT4. *Front. Biosci.* 8:d620–d641.

Hashiramoto, M., and D.E. James. 2000. Characterization of insulin-responsive GLUT4 storage vesicles isolated from 3T3-L1 adipocytes. *Mol. Cell. Biol.* 20:416–427.

Higuchi, H., and S.A. Endow. 2002. Directionality and processivity of molecular motors. *Curr. Opin. Cell Biol.* 14:50–57.

Holman, G.D., L. Lo Leggio, and S.W. Cushman. 1994. Insulin-stimulated GLUT4 glucose transporter recycling. A problem in membrane protein subcellular trafficking through multiple pools. *J. Biol. Chem.* 269: 17516–17524.

Inoue, M., L. Chang, J. Hwang, S.H. Chiang, and A.R. Saltiel. 2003. The exocyst complex is required for targeting of Glut4 to the plasma membrane by insulin. *Nature.* 422:629–633.

Karylowski, O., A. Zeigerer, A. Cohen, and T.E. McGraw. 2004. GLUT4 is retained by an intracellular cycle of vesicle formation and fusion with endosomes. *Mol. Biol. Cell.* 15:870–882.

Lampson, M.A., J. Schmoranzer, A. Zeigerer, S.M. Simon, and T.E. McGraw. 2001. Insulin-regulated release from the endosomal recycling compartment is regulated by budding of specialized vesicles. *Mol. Biol. Cell*. 12: 3489–3501.

Lee, W., J. Ryu, R.P. Souto, P.F. Pilch, and C.Y. Jung. 1999. Separation and partial characterization of three distinct intracellular GLUT4 compartments in rat adipocytes. Subcellular fractionation without homogenization. *J. Biol. Chem.* 274:37755–37762.

Li, C.H., L. Bai, D.D. Li, S. Xia, and T. Xu. 2004. Dynamic tracking and mobility analysis of single GLUT4 storage vesicle in live 3T3-L1 cells. *Cell Res.* 14:480–486.

Loerke, D., W. Stuhmer, and M. Oheim. 2002. Quantifying axial secretory-granule motion with variable-angle evanescent-field excitation. *J. Neurosci. Methods.* 119:65–73.

Ma, S., and R.L. Chisholm. 2002. Cytoplasmic dynein-associated structures move bidirectionally in vivo. *J. Cell Sci.* 115:1453–1460.

Malide, D., and S.W. Cushman. 1997. Morphological effects of wortmannin on the endosomal system and GLUT4-containing compartments in rat adipose cells. *J. Cell Sci.* 110:2795–2806.

Malide, D., N.K. Dwyer, E.J. Blanchette-Mackie, and S.W. Cushman. 1997. Immunocytochemical evidence that GLUT4 resides in a specialized translocation post-endosomal VAMP2-positive compartment in rat adipose cells in the absence of insulin. *J. Histochem. Cytochem.* 45:1083–1096.

Malide, D., G. Ramm, S.W. Cushman, and J.W. Slot. 2000. Immunoelectron microscopic evidence that GLUT4 translocation explains the stimulation of glucose transport in isolated rat white adipose cells. *J. Cell Sci.* 113: 4203–4210.

Martin, S., J. Tellam, C. Livingstone, J.W. Slot, G.W. Gould, and D.E. James. 1996. The glucose transporter (GLUT-4) and vesicle-associated membrane protein-2 (VAMP-2) are segregated from recycling endosomes in insulin-sensitive cells. *J. Cell Biol.* 134:625–635.

Oatey, P.B., D.H. Van Weering, S.P. Dobson, G.W. Gould, and J.M. Tavare.

1997. GLUT4 vesicle dynamics in living 3T3 L1 adipocytes visualized with green-fluorescent protein. *Biochem. J.* 327:637–642.

Patki, V., J. Buxton, A. Chawla, L. Lifshitz, K. Fogarty, W. Carrington, R. Tuft, and S. Corvera. 2001. Insulin action on GLUT4 traffic visualized in single 3T3-l1 adipocytes by using ultra-fast microscopy. *Mol. Biol. Cell.* 12:129–141.

Pessin, J.E., D.C. Thurmond, J.S. Elmendorf, K.J. Coker, and S. Okada. 1999. Molecular basis of insulin-stimulated GLUT4 vesicle trafficking. Location! Location! Location! *J. Biol. Chem.* 274:2593–2596.

Rea, S., and D.E. James. 1997. Moving GLUT4: the biogenesis and trafficking of GLUT4 storage vesicles. *Diabetes.* 46:1667–1677.

Saltiel, A.R., and J.E. Pessin. 2003. Insulin signaling in microdomains of the plasma membrane. *Traffic.* 4:711–716.

Satoh, S., H. Nishimura, A.E. Clark, I.J. Kozka, S.J. Vannucci, I.A. Simpson, M.J. Quon, S.W. Cushman, and G.D. Holman. 1993. Use of bismannose photolabel to elucidate insulin-regulated GLUT4 subcellular trafficking kinetics in rat adipose cells. Evidence that exocytosis is a critical site of hormone action. *J. Biol. Chem.* 268:17820–17829.

Schmoranzer, J., and S.M. Simon. 2003. Role of microtubules in fusion of post-Golgi vesicles to the plasma membrane. *Mol. Biol. Cell.* 14:1558–1569.

Schmoranzer, J., M. Goulian, D. Axelrod, and S.M. Simon. 2000. Imaging constitutive exocytosis with total internal reflection fluorescence microscopy. *J. Cell Biol.* 149:23–32.

Semiz, S., J.G. Park, S.M. Nicoloro, P. Furcinitti, C. Zhang, A. Chawla, J. Leszyk, and M.P. Czech. 2003. Conventional kinesin KIF5B mediates insulin-stimulated GLUT4 movements on microtubules. *EMBO J.* 22: 2387–2399.

Slot, J.W., H.J. Geuze, S. Gigengack, G.E. Lienhard, and D.E. James. 1991. Immuno-localization of the insulin regulatable glucose transporter in brown adipose tissue of the rat. *J. Cell Biol.* 113:123–135.

Suzuki, K., and T. Kono. 1980. Evidence that insulin causes translocation of glucose transport activity to the plasma membrane from an intracellular storage site. *Proc. Natl. Acad. Sci. USA.* 77:2542–2545.

Tengholm, A., and T. Meyer. 2002. A PI3-kinase signaling code for insulin-triggered insertion of glucose transporters into the plasma membrane. *Curr. Biol.* 12:1871–1876.

Timmers, K.I., A.E. Clark, M. Omatsu-Kanbe, S.W. Whiteheart, M.K. Bennett, G.D. Holman, and S.W. Cushman. 1996. Identification of SNAP receptors in rat adipose cell membrane fractions and in SNARE complexes coimmunoprecipitated with epitope-tagged N-ethylmaleimide-sensitive fusion protein. *Biochem. J.* 320:429–436.

Vega, F.V., and T. Kono. 1979. Sugar transport in fat cells: effects of mechanical agitation, cell-bound insulin, and temperature. *Arch. Biochem. Biophys.* 192:120–127.

Watson, R.T., A.H. Khan, M. Furukawa, J.C. Hou, L. Li, M. Kanzaki, S. Okada, K.V. Kandror, and J.E. Pessin. 2004. Entry of newly synthesized GLUT4 into the insulin-responsive storage compartment is GGA dependent. *EMBO J.* 23:2059–2070.

Zeigerer, A., M.A. Lampson, O. Karylowski, D.D. Sabatini, M. Adesnik, M. Ren, and T.E. McGraw. 2002. GLUT4 retention in adipocytes requires two intracellular insulin-regulated transport steps. *Mol. Biol. Cell*. 13: 2421–2435.

Zimmerberg, J., R. Blumenthal, D.P. Sarkar, M. Curran, and S.J. Morris. 1994. Restricted movement of lipid and aqueous dyes through pores formed by influenza hemagglutinin during cell fusion. *J. Cell Biol.* 127:1885–1894.

Lizunov et al. http://www.jcb.org/cgi/doi/10.1083/jcb.200412069

Detection of GLUT4 release to the PM by immunofluorescence

Upon insulin stimulation the cells became immunostained with anti-HA antibodies known not to enter the intact PM (Dawson et al., 2001). The HA-tagged exofacial domain of GLUT4 originally exposes to the GLUT4 vesicle lumen and only becomes accessible to the antibodies in the extracellular media if the GLUT4 vesicles fuse with the PM. Accordingly, and consistent with the earlier observations (Malide et al., 1997; Dawson et al., 2001), when the cells were incubated with insulin for 5–15 min at 37°C degree before immunostaining, HA immunofluorescence (Fig. S2 A, red) became highly colocalized with GFP fluorescence of GLUT4 (Fig. S2 A). In contrast, when the cells were first pretreated for 10 min with 100 nM wortmannin, which is known to inhibit insulin signaling, GFP fluorescence showed a punctate pattern with no colocalization with anti-HA immunofluorescence (Fig. S2 B).

FRAP measurements of GLUT-GFP lateral mobility in the PM

Bleaching of GLUT-GFP confined in the TIRF area was performed by turning laser power to the maximum (70 mW). Radius of the circular area of the cell subjected to TIRF depended on the level of squeezing of each particular cell between the coverslips, and varied from 10 to 30 μm. More than 80% of initial fluorescence was bleached out in 3 s. After that, laser power was set to the minimum of level (6 mW) and, with the shutter opening every 15 s, snapshots of TIRF area were acquired for 5–10 min. Stacks of images were further transferred to ImageJ and processed as described below. Mean gray value of the circular ROI representing bleached TIRF area of the cell was calculated for each image and plotted versus time. The experimental data was fitted with a theoretical curve (Axelrod et al., 1976; Soumpasis, 1983; Klein et al., 2003) using the least square algorithm in Maple software (Maplesoft): $F(t) = F_0 + (F_\infty - F_0)e^{(-2\tau/t)}[I_0(2\tau/t) + I_1(2\tau/t)]$, where t is the time, τ is the fitting parameter, F_0 is the fluorescence intensity of the bleached area immediately after bleaching; F_∞ is the fluorescence intensity of the bleached area after recovery to the constant level. I_0 and I_1 are modified Bessel functions. Characteristic time τ obtained from fitting procedure was used to calculate lateral diffusion coefficient for GLUT-GFP from the formula: $D = R^2/4\tau$, where R is the radius of the bleached area.

Kinetic analysis of GLUT4 recycling in primary adipose cells

In adipose cells, GLUT4 cycles between the following main locations (Holman et al., 1994; Lee et al., 1999; Bryant et al., 2002): (a) GLUT4 vesicles (constituting the GLUT4-releasable pool); (b) the rest of subcellular GLUT4 that is not directly delivered to the PM upon insulin stimulation (mainly "endosomal" GLUT4); and (c) GLUT4 associated with the PM, i.e., GLUT4 exposed to the extracellular medium and thus accessible for antibody labeling. The basal distribution of GLUT4 among these three general pools is highly dependent on the experimental system under consideration. In freshly prepared isolated rat adipose cells, most of the GLUT4 is found in the GLUT4 vesicles and little in either the "endosomal" pool or PM; in 3T3-L1 adipocytes, intracellular GLUT4 is roughly divided between the GLUT4 vesicles and the "endosomal" pool, with little in PM; and as reported here and previously (Malide et al., 1997), in primary rat adipose cells cultured for increasing periods, the distribution shifts with culture duration from that observed in the freshly prepared cells to one quite similar to that observed in the 3T3-L1 adipocytes. As noted in the text, we have performed the present TIRFM studies under conditions such that the basal GLUT4 distribution approximates that in freshly prepared cells despite requiring culture times sufficient to provide adequate HA-GLUT4-GFP expression for visualization.

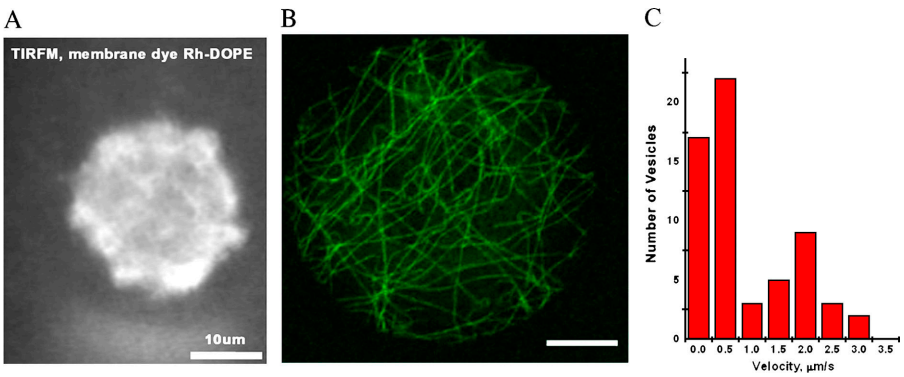

Figure S1. **TIRF-zone geometry, microtubular network and vesicle velocity distribution in adipose cells in the basal state.** (A) TIRFM image of the PM in the TIRF-zone labeled with lipid fluorescent probe phosphatidylethanolamine-lissamine rhodamine B; the entire region of the PM in the TIRF-zone is visible under TIRFM. (B) Cells transfected with GFP-tubulin show an extensive microtubular network that covers the entire cytoplasm. Thin confocal sections were taken every 200 nm through the flattened bottom region of the cell (the same that was used for TIRFM) and then were three-dimensionally reconstructed to visualize the complete microtubular network within the monitored region. Note that many microtubules are sufficiently long (>10 μm) to account for the fast liner movements of the GLUT4 vesicles. (C) Distribution of GLUT4 vesicle velocity, estimated from linear displacements of vesicles recorded on TIRFM time-lapse videos. Note that the distribution exhibits two peaks: 0.6 and 2 μm/s. Bars, 10 μm.

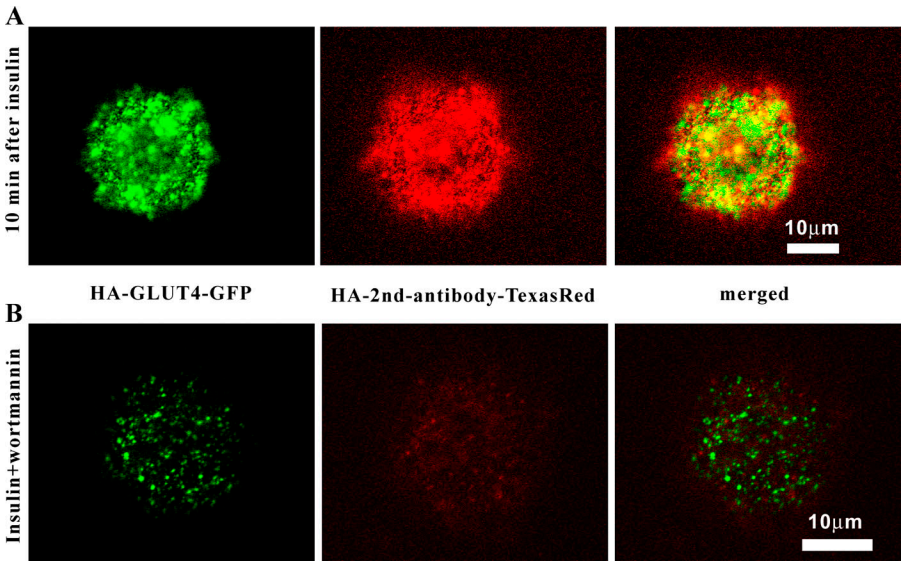

Figure S2. **Immunostaining of HA-GLUT4-GFP on the PM of insulin-stimulated adipose cells and effect of wortmannin.** (A) Cells were incubated with 67 nM insulin for 10 min at 37°C and fixed without permeabilization of the plasma membrane. Cells show high membrane staining with anti-HA antibody visualized with second antibody Texas red. Note high colocalization of immunofluorescence (red) with GFP fluorescence (green). (B) Cells treated with wortmannin and incubated with insulin at the same conditions. Note low immunofluorescence staining and punctate pattern of GLUT4-GFP fluorescence resembling the basal state distribution (as in Fig. 1 C).

A 3-pool model is the minimal one describing the behavior of GLUT4 in rat adipose cells (Holman et al., 1994); moreover, the steady-state distribution of GLUT4 between the three pools described above is consistent with morphological observations (Malide et al., 1997). We extend this model to account for GLUT4 mobility; thus, subdividing GLUT4 vesicles into moving and stationary pools. The vesicle is considered moving if it makes a detectable path (see Fig. 1, A and C). The scheme of this 4-pool model is presented in Fig. S4 A. The following GLUT4 pools are considered: (1) pool 1, GLUT4 in vesicles moving in the TIRF zone; (2) pool 2, GLUT4 in vesicles that remain static in the TIRF zone; (3) pool 3, GLUT4 in the PM or in vesicles fused with the PM so that the GLUT4 is fully exposed to the extracellular medium and accessible to extracellular antibodies; (4) pool 4, the rest of subcellular GLUT4.

As GLUT4 vesicles are uniformly distributed near the PM (see Fig. 1), we assume that the number of GLUT4 vesicles (both moving and stationary) in the TIRF zone is directly proportional to the total number of GLUT4 vesicles in a cell. The same holds for the PM GLUT4. Thus, the dynamics of the fraction of the GLUT4 visible in the TIRF zone correctly represents the overall dynamics of the GLUT4 in the whole adipose cell. Accordingly, we consider the behavior of a fraction of GLUT4, C, corresponding to a single TIRF zone. This fraction is distributed between the four pools described above so that $C1 + C2 + C3 + C4 = C$ and C remains constant. For simplicity, we assume that $C = 1$. The system of equations describing GLUT4 dynamics is as follows (System 1):

$$\cdot C1(t) = -k1C1 + k2C2 + k5C$$

$$\cdot C2(t) = -(k2 + k3)C2 + k1C$$

$$\frac{}{t} C3(t) = -k4C3 + k3C$$

$$\frac{}{t} C4(t) = -k5C4 + k4C$$

$$C1 + C2 + C3 + C4 =$$

The steady-state distribution of GLUT4 is determined from a system of three algebraic equations (System 2):

$$C1C1 + k2C2 + (1 - C1 - C2 - C3)k5 =$$

$$(k2 + k3)C2 + k1C1 =$$

$$\cdot k4C3 + k3C2 =$$

Basal steady-state

From the literature, we know that ~5% of GLUT4 is in the PM (i.e., $C3 = 0.05$) and that the endocytosis rate constant $k4 = 0.06$ min^{-1} (Holman et al., 1994, Malide et al., 2000); from our data, we obtain $C1/C2$, $k1$, and $k2$ (see Table S1). The 3 remaining unknowns, $-k3$, $k5$, and $C1$, are defined by solving the System 2 equations.

Table S1. **The parameters of the kinetic model and steady-state distrbution of GLUT4**

	Basal	Stimulated
$k1$[a]	1/15	1/5
$k2$	1/150	1/150
$k3$	1/15000	1/600
$k4$	10^{-3}	10^{-3}
$k5$	10^{-2}	10^{-2}
$C1$ (GLUT4 moving)	0.08	0.01
$C2$ (GLUT4 stationary)	0.85	0.34
$C3$ (PM)	0.05	0.58
$C4$(subcellular rest)	0.02	0.07

$k1$ is estimated from the mean distance <l> the vesicle passes before getting tethered for the first time: $k1 \sim <V>/<l>$, where <V> is the mean vesicle velocity (approximated as 1 μm/s from Fig. S3), and <l> = 15 (15 ± 6) μm in the basal state and 5 (5 ± 2) μm in the insulin-stimulated state, respectively (see Fig. 3 D). $k2$ in the basal state is estimated from the ratio of mobile/stationaty vesicles: $k2 = k1^{a}(C2/C1)$ provided that $k3$ is significantly smaller than $k2$; $C2/C1$ obtained experimentally is ~10 ($C2/C1 = (N_{total} - N_{moving})/N_{moving} \sim 14/1.4$ where N_{total} is the number of GLUT4 vesicles detected in a ROI of 100 μm^2 randomly selected in a snapshot of the TIRF zone and N_{moving} is the number of moving vesicles in a ROI of the same area (the numbers were averaged over 20 different cells). We note that while at each moment many vesicles are stationary, in the basal state the attachment to the PM is mostly reversible: vesicles will continue moving until they reach the fusion site on the PM as each GLUT4 molecule ultimately cycles through the PM. $C1$ and $C2$: in the basal state, more than 90% of GLUT4 is sequestered subcellularly and this GLUT4 fails to colocalize with endosomal markers (Malide et al., 1997) indicating that it is all sequestered in specialized GLUT4 vesicles; correspondingly, we detected no colocalization of GLUT4 and FM4-64 taken up by adipose cells in the basal state (unpublished data).

[a]Rate constants are s^{-1}.

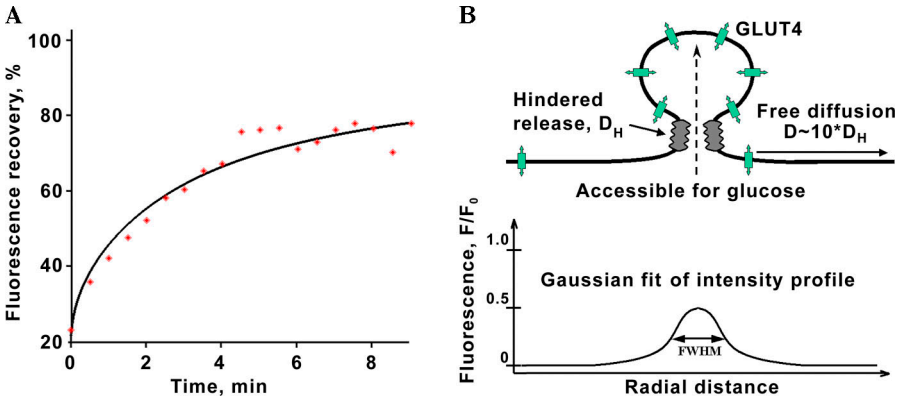

Figure S3. **GLUT4 lateral diffusion estimated by FRAP and by release from fusing vesicles in adipose cells.** (A) GLUT4-GFP fluorescence recovery (red) in a circular region of the PM (10 μm radius), bleached ~15 min after insulin stimulation. Black curve represents theoretical fit with characteristic time of recovery τ = 180 s, giving an estimate of GLUT4 diffusion coefficient: D = 0.14 $\mu m^2/s$. (B) Cartoon illustrating the constrained release of GLUT4 from fusing GLUT4 vesicles. The 10-fold difference of the average observed time of GLUT4 release from the expected time of free diffusion can be accounted by fusion pore constrains (D_H, the rate-limiting diffusion of GLUT4 molecules through the fusion pore). Bottom panel shows lack of widening of the fluorescence profile of a fusing vesicle if diffusion through the pore is significantly slower than diffusion in the plasma membrane.

Insulin steady state

From the literature, we know that ~50% of GLUT4 is translocated to the PM (*C3*) and ~30% remain in GLUT4 vesicles (*C*1 + *C*2) and that *k*4 remains equal to 0.06 min^{-1} (Holman et al., 1994, Malide et al., 2000); from our data, we measure changes in *k*1 (see Table S1). So the unknowns are *k*2, *k*3, *k*5, and *C*1 (or *C*2). They cannot all be determined from the System 2 equations, so we assume that *k*5 remains unchanged and find approximate steady-state values for the remaining unknowns. To verify the assumption, we fit the kinetics of the increase of PM GLUT4 (and the respective reduction of vesicular GLUT4, see Fig. S4, B and C) upon insulin stimulation (solving the System 1 equations using the matrix exponent method) and find that the kinetics are indeed well described assuming that only *k*1 and *k*3 are changed by insulin. If *k*3 is assumed to remain unchanged, the model does not describe either the kinetics of the insulin response or the steady-state distribution of GLUT4 in the insulin-stimulated state.

Conclusion

We conclude that insulin primarily increases the probability of tethering and also stimulates priming of vesicles tethered to specific fusion sites on the PM. This conclusion is well supported by biochemical kinetic data obtained using rat adipose cells.

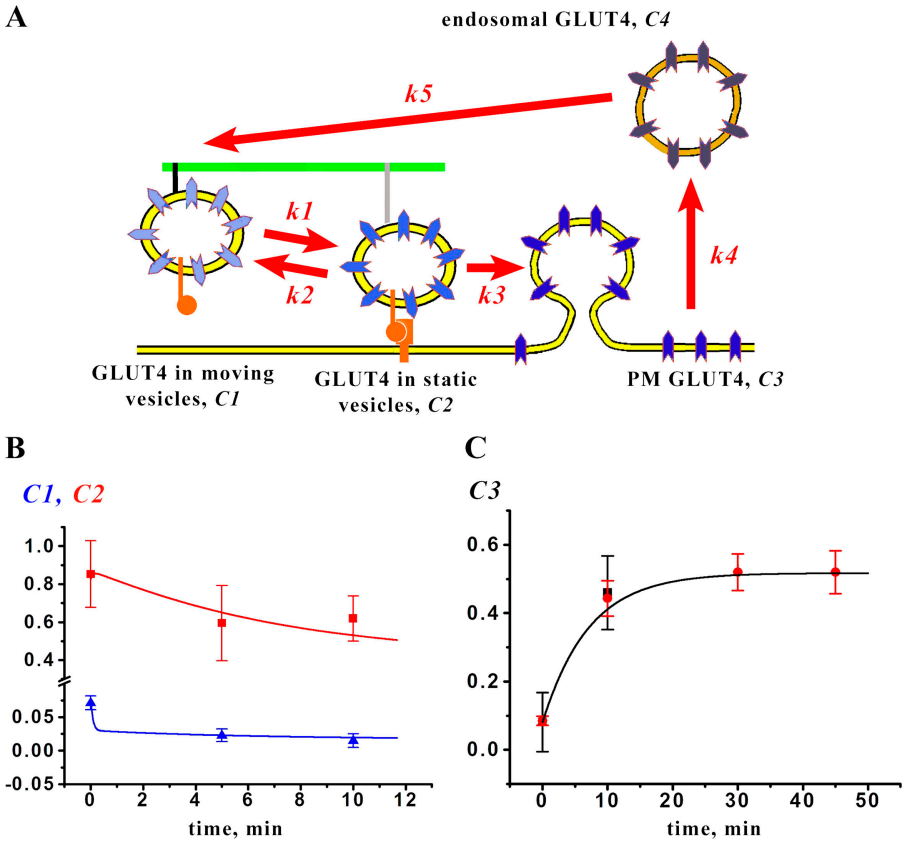

Figure S4. **Model of GLUT4 recycling in primary adipose cells.** (A) Scheme illustrating GLUT4 recycling in a 4-pool model. (B) Changes in the number of moving (blue) and static (red) GLUT4 vesicles upon insulin stimulation. Experimental data are shown by symbols with error bars (the number of vesicles was normalized to correspond to the fraction of GLUT4 vesicles in each corresponding pool); the curves were generated by the model shown in A, taking the basal initial values of *C*1 and *C*2, and assuming that at *t* = 0 and *k*1 and *k*3 instantaneously change to their values characteristic for the insulin-stimulated state. (C) Changes in PM GLUT4 upon insulin stimulation. Experimental data are shown by symbols with error bars; changes are shown in total fluorescence of the TIRF zone corresponding to fusing GLUT4 vesicles (black) and the kinetics of the antibody labeling of PM GLUT4 (red, taken from Dawson et al. [2001]). The initial basal values of C3 and the instantaneous change of *k*1 and *k*3 in response to insulin are assumed as in B.

References

Axelrod, D., D.E. Koppel, J. Schlessinger, E. Elson, and W.W. Webb. 1976. Mobility measurement by analysis of fluorescence photobleaching recovery kinetics. *Biophys. J.* 16:1055–1069.

Bryant, N.J., R. Govers, and D.E. James. 2002. Regulated transport of the glucose transporter GLUT4. *Nat. Rev. Mol. Cell Biol.* 3:267–277.

Dawson, K., A. Aviles-Hernandez, S.W. Cushman, and D. Malide. 2001. Insulin-regulated trafficking of dual-labeled glucose transporter 4 in primary rat adipose cells. *Biochem. Biophys. Res. Commun.* 287:445–454.

Holman, G.D., L. Lo Leggio, and S.W. Cushman. 1994. Insulin-stimulated GLUT4 glucose transporter recycling. A problem in membrane protein subcellular trafficking through multiple pools. *J. Biol. Chem.* 269:17516–17524.

Klein, C., T. Pillot, J. Chambaz, and B. Drouet. 2003. Determination of plasma membrane fluidity with a fluorescent analogue of sphingomyelin by FRAP measurement using a standard confocal microscope. *Brain Res. Brain Res. Protoc.* 11:46–51.

Lee, W., J. Ryu, R.P. Souto, P.F. Pilch, and C.Y. Jung. 1999. Separation and partial characterization of three distinct intracellular GLUT4 compartments in rat adipocytes. Subcellular fractionation without homogenization. *J. Biol. Chem.* 274:37755–37762.

Malide, D., N.K. Dwyer, E.J. Blanchette-Mackie, and S.W. Cushman. 1997. Immunocytochemical evidence that GLUT4 resides in a specialized translocation post-endosomal VAMP2-positive compartment in rat adipose cells in the absence of insulin. *J. Histochem. Cytochem.* 45:1083–1096.

Malide, D., G. Ramm, S.W. Cushman, and J.W. Slot. 2000. Immunoelectron microscopic evidence that GLUT4 translocation explains the stimulation of glucose transport in isolated rat white adipose cells. *J. Cell Sci.* 113:4203–4210.

Soumpasis, D.M. 1983. Theoretical analysis of fluorescence photobleaching recovery. *Biophys. J.* 41:95–97.